HOKKAIDO UNIVERSITY

Title	Isotopic compositions of asteroidal liquid water trapped in fluid inclusions of chondrites
Author(s)	Yurimoto, Hisayoshi; Itoh, Shoichi; Zolensky, Michael et al.
Citation	Geochemical Journal, 48(6), 549-560 https://doi.org/10.2343/geochemj.2.0335
Issue Date	2014
Doc URL	https://hdl.handle.net/2115/57641
Type	journal article
File Information	GJ_48_549-.pdf

Hokkaido University Collection of Scholarly and Academic Papers : HUSCAP

Geochemical Journal, Vol. 48, pp. 549 to 560, 2014 doi:10.2343/geochemj.2.0335

Isotopic compositions of asteroidal liquid water trapped in fluid inclusions of chondrites

HISAYOSHI YURIMOTO,[1,2]* SHOICHI ITOH,[1]** MICHAEL ZOLENSKY,[3] MINORU KUSAKABE,[4] AKIYA KAREN[5] and ROBERT BODNAR[6]

[1]Department of Natural History Sciences, Hokkaido University, Sapporo 060-0810, Japan
[2]Isotope Imaging Laboratory, Creative Research Institution, Hokkaido University, Sapporo 001-0021, Japan
[3]Astromaterials Research and Exploration Science, KT, NASA Johnson Space Center, Houston, TX 77058, U.S.A.
[4]Department of Environmental Biology and Chemistry, The University of Toyama, Gofuku 3190, Toyama 930-8555, Japan
[5]Toray Research Center, Inc., 3-7, Sonoyama 3-chome, Otsu, Shiga 520-8567, Japan
[6]Department of Geosciences, 4044 Derring Hall, Virginia Tech, Blacksburg, VA 24061 U.S.A.

(*Received June 2, 2014; Accepted September 17, 2014*)

Determination of isotopic composition of extraterrestrial liquid water provides important information regarding the origin of water on Earth and the terrestrial planets. Fluid inclusions in halite of ordinary chondrites are the only direct samples of extraterrestrial liquid water available for laboratory measurements. We determined H and O isotopic compositions of this water by secondary ion mass spectrometry equipped with a cryogenic apparatus for sample cooling. Isotopic compositions of the fluid inclusion fluids (brines) were highly variable among individual inclusions, $-400 < \delta D < +1300‰$; $-20 < \Delta^{17}O < +30‰$, indicating that these aqueous fluids were in isotopic disequilibrium before trapping in halite on asteroids. The isotopic variation of fluids shows that various degrees of water-rock interaction had been underway on the asteroids before trapping between D-rich-^{16}O-poor aqueous fluid, D-poor-^{16}O-rich aqueous fluid, and asteroidal rock by delivery of cometary water onto hydrous asteroids. This may be a fundamental mechanism in the evolution of modern planetary water.

Keywords: fluid inclusion, hydrogen isotope, oxygen isotope, asteroid, water

INTRODUCTION

The origin of the water of terrestrial planets remains one of the primary issues of planetary sciences. It is believed that terrestrial planets formed inside of the water ice evaporation line (snow line) in the solar nebula (Hayashi *et al*., 1985) where it was difficult to trap water components. It is useful to use isotopic compositions as a tracer in order to discuss the origin and evolution of materials, but we have little knowledge of isotopic compositions of extraterrestrial water components. In particular, there is no report of isotopic compositions of extraterrestrial liquid water.

Aqueous fluid inclusions contained within crystals of halite in two ordinary chondrites are the only extraterrestrial liquid water samples available for laboratory measurements (Zolensky *et al*., 1999). Because chondrites are primitive materials in the solar system and chondrite-like materials formed the terrestrial planets, isotopic compositions of chondritic liquid water provide a direct evidence to reveal the origin of water of terrestrial planets. The fluid inclusions were found in halite (NaCl) and sylvite (KCl) (hereafter collectively called "halite") from two ordinary chondrite regolith breccias (Monahans (1998), hereafter simply "Monahans" (H5), and Zag (H3-6)) (Rubin *et al*., 2002; Zolensky *et al*., 1999, 2000). Both meteorites contain millimeter to centimeter-sized aggregates of blue to purple halite containing aqueous fluid inclusions in the matrix. The halite grains were dated by K–Ar, Rb–Sr and I–Xe systematics to be ~4.5 Ga (Bogard *et al*., 2001; Whitby *et al*., 2000; Zolensky *et al*., 1999), and thus the trapped aqueous fluids are at least as ancient. These halite grains are blue to purple owing to the gradual accumulation of trapped electrons in cation vacancies (Nassau, 1983), resulting, probably, from the beta decay of ^{40}K. Since recently recrystallized halite would be colorless, fluid within the colored halite grains must be pre-terrestrial in origin. Heating/freezing studies of the fluid inclusions in Monahans halite grains demonstrated that they were trapped at approximately 25°C (Zolensky *et al*., 1999), and their presence in the halite requires their

*Corresponding author (e-mail: yuri@ep.sci.hokudai.ac.jp)
**Present address: Department of Earth and Planetary Sciences, Kyoto University, Kyoto 606-8502, Japan.

Copyright © 2014 by The Geochemical Society of Japan.

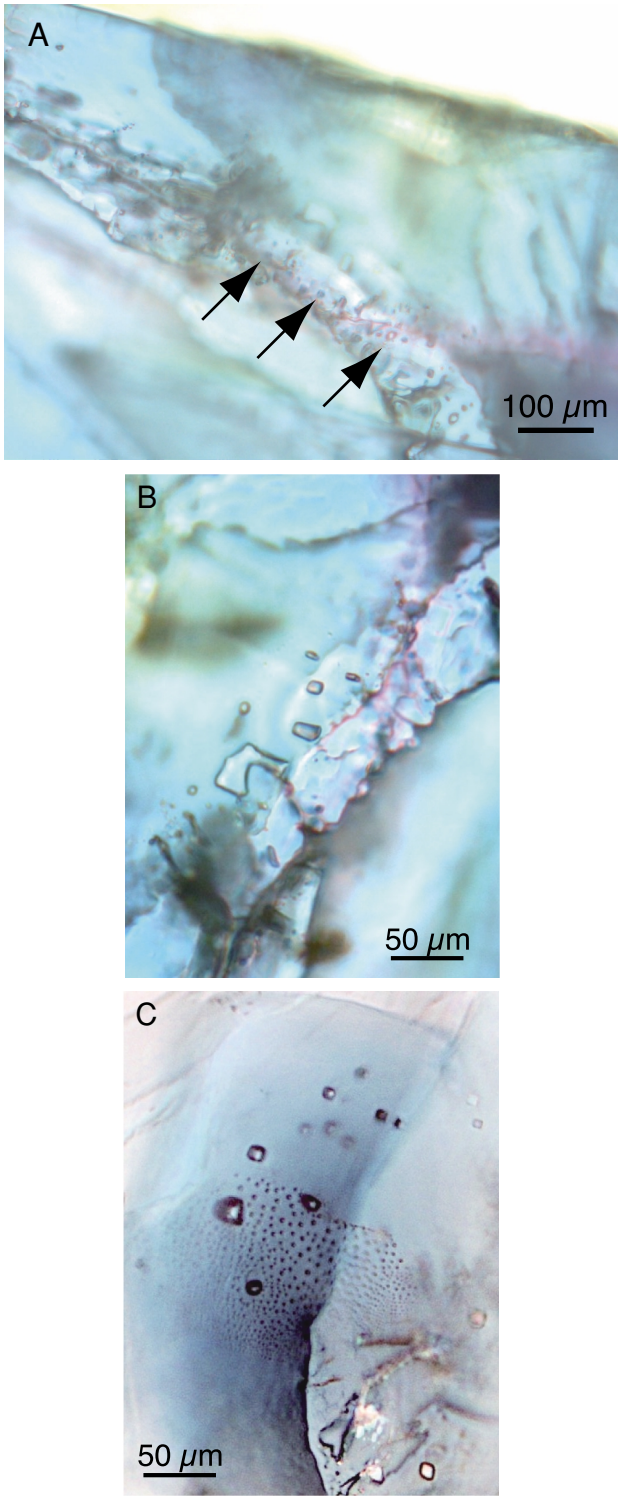

Fig. 1. Representative photographs of fluid inclusions in halite crystals (A) Distributions of fluid inclusions in halite of Monahans (1998). Arrows point to several inclusions. (B) Fluid inclusions in Monahans halite. (C) Fluid inclusions in Zag halite.

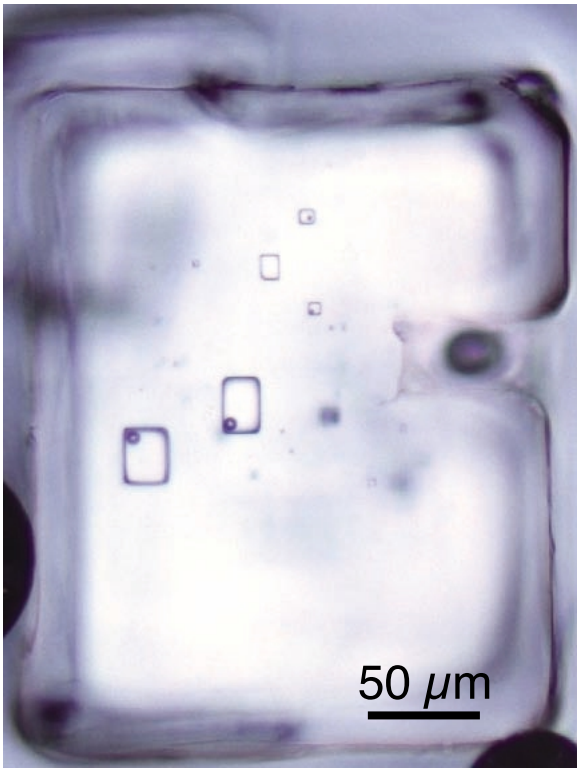

Fig. 2. Photomicrograph of synthetic fluid inclusions in halite.

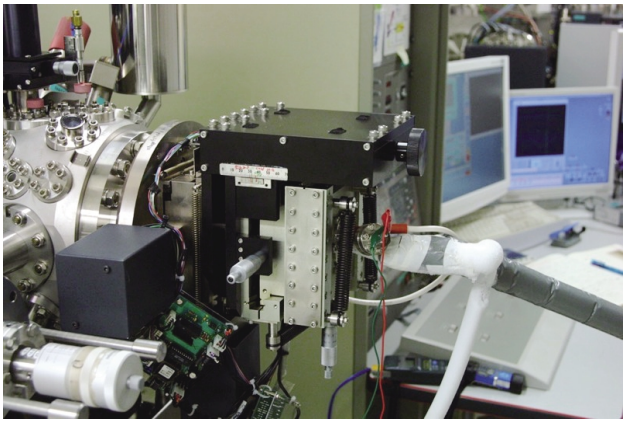

Fig. 3. Cryo-sample-stage installed on Cameca ims-1270. The temperature of the sample stage is cooled by liquid nitrogen, which is supplied by the frost-covered (white) tube.

incorporation into the H chondrite asteroid after metamorphism, as heating would have released fluids from halite.

Large variations of hydrogen isotopic composition have been observed in hydrous minerals from chondrites (Robert, 2006). Cometary and interstellar water is highly D-enriched (Butner *et al*., 2007; Villanueva *et al*., 2009),

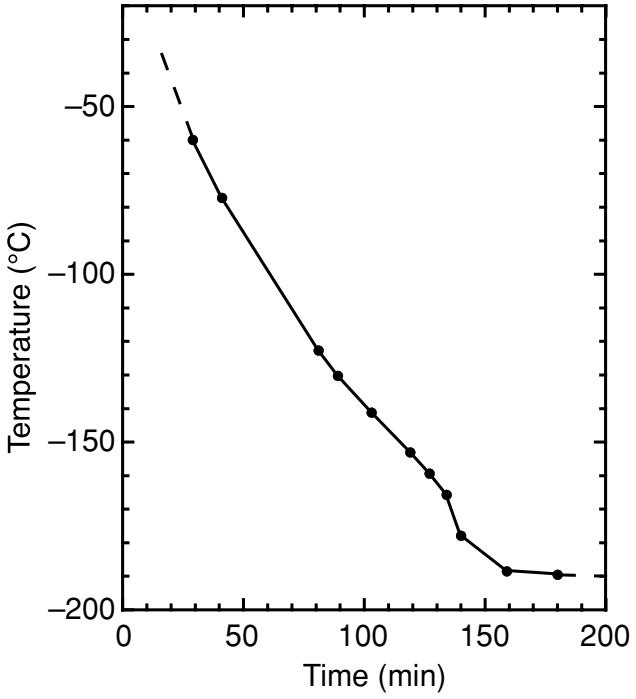

Fig. 4. Cooling temperature curve of cryo-sample-stage as a function of time after supplying liquid nitrogen from room temperature.

representing cloud or outer solar disk chemistry. The hydrogen isotopic composition of hydrous minerals in chondrites is believed to reflect inner solar system water (Alexander *et al*., 2012; Robert, 2006).

Oxygen isotopes in the solar system are also highly variable (Sakamoto *et al*., 2007; Yurimoto *et al*., 2008), reflecting contributions of an H_2O component (Kuramoto and Yurimoto, 2005; Lyons and Young, 2005; Yurimoto and Kuramoto, 2004). However, it is impossible to measure isotopes of hydrogen and oxygen simultaneously in hydrous minerals, because they invariably contain structural oxygen not bound in water. Halite contains no structural oxygen or hydrogen, allowing the isotopic composition of oxygen and hydrogen in aqueous fluid inclusions to be measured. Thus, fluid inclusions in halite have the potential to reveal unique information regarding the origin and activity of aqueous fluids in the early solar system. This information contains, and perhaps uniquely identifies, the source of the aqueous fluid from which the halite precipitated.

Here we report direct measurement of the hydrogen and oxygen isotopic compositions of the aqueous fluid in halite fluid inclusion by cryo-secondary ion mass spectrometry (Cryo-SIMS), and discuss the origin of this water. Preliminary results have been presented in Yurimoto *et al*. (2010).

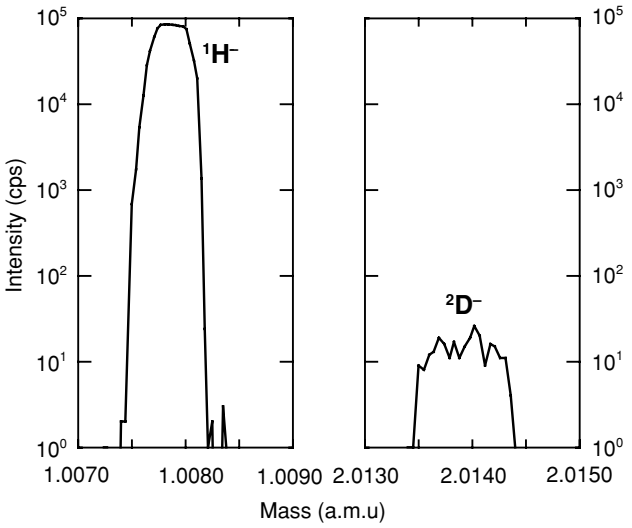

Fig. 5. Representative mass spectra of hydrogen isotopes of a fluid inclusion standard.

EXPERIMENTAL

Sample preparation

We have determined oxygen and hydrogen isotopic compositions of fluid inclusion fluids in halite crystals from Monahans (1998) H5 and Zag H3-6 ordinary chondrites. Both meteorites used in this study were recovered immediately upon falling and preserved under dry nitrogen, limiting terrestrial alteration. These samples have never been exposed to terrestrial liquid water. The halite crystals of 0.1 to 1 mm in size were picked from fresh fracture surfaces of the chondrites by a stainless needle. We carefully observed each halite crystal surfaces under an optical microscope and selected crystals having fluid inclusions within several tens of micrometers below the surface for isotope analysis (Fig. 1).

Synthesis of fluid inclusion standard

We prepared synthetic fluid inclusions with known isotopic compositions in halite crystals as standards in order to calibrate measured δ-values. An ion-exchanged pure water was prepared from meteoric water of Sapporo, Japan. Isotope ratios of the pure water were determined by conventional gas mass spectrometry (Kusakabe and Matsuhisa, 2008) as $\delta^{18}O_{SMOW} = -11.17(6)‰$, $\delta^{17}O_{SMOW} = -5.81(3)‰$ and $\delta D = -76.7(5)‰$. The pure water added with supersaturated level of ground NaCl powder (JIS K 8150, Kanto Chemical Co., Inc.) was bottled up into a 125 ml polyethylene bottle and placed for three months on a windowsill in a laboratory room. Millimeter sized halite crystals were recrystallized on the bottom of the bottle. The precipitating crystals trapped nanoliter-sized quantities of the solution as fluid inclusions. Because the

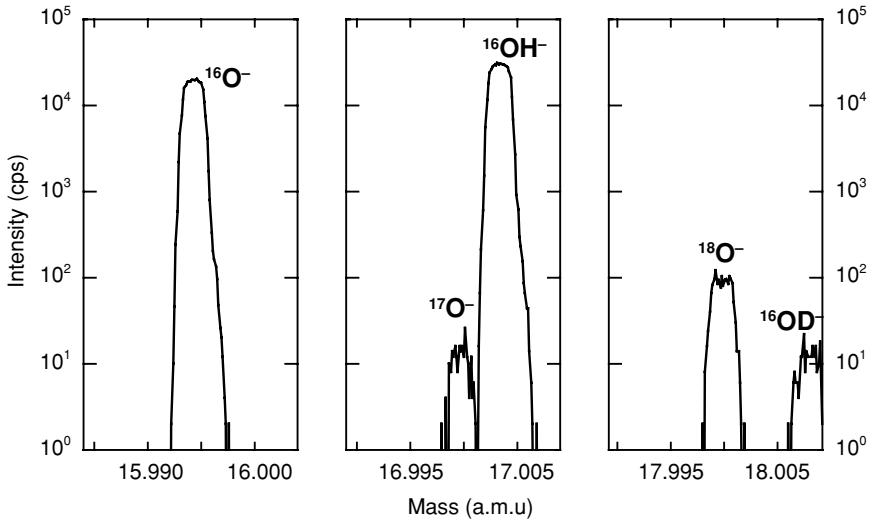

Fig. 6. Representative mass spectra of oxygen isotopes of a fluid inclusion standard.

crystal growth occurred in closed system, the isotopic compositions of the trapped water must be the same as those of the pure water. We selected appropriate halite crystals having fluid inclusions within several of tens micrometers below the surface to be used as standards to calibrate the isotopic compositions of fluid inclusions in the meteorite halite (Fig. 2).

Measurement condition of secondary ion mass spectrometry (SIMS)

The halite crystals to be analyzed were fastened to a silicon wafer by epoxy, with the surface with fluid inclusions positioned on top. A 30 nm thick Au layer was deposited on the sample surface by ion beam sputter deposition in order to load secondary acceleration voltages and reduce electrostatic charging of the sample surface during analysis. The sample was mounted on a sample holder of a Cameca ims-1270 instrument with the top surface of halite set along the top plane of the sample holder.

The isotopic measurement of individual aqueous fluid inclusions in halite requires a secondary ion mass spectrometer equipped with a cryo-sample-stage, which is not a typical instrument configuration. A Cameca ims-1270 SIMS instrument equipped with a cryo-sample-stage at Hokkaido University was prepared for the measurements. The cryo-sample-stage (Techno. I. S. Corporation) was placed in the sample chamber in place of the original sample stage (Fig. 3) and cooled down to about –190°C using liquid nitrogen (Fig. 4). At this temperature the aqueous fluid (a brine) in fluid inclusions was frozen. The operating vacuum in the sample chamber was maintained at less than 2×10^{-9} Torr.

A Cs^+ beam of 15 keV was used as primary beam and negative secondary ions of –5 keV were extracted into the mass spectrometer. A normal incident electron gun was applied to compensate positive charging of the sputtered region due to primary beam irradiation. The primary beam of 10 to 15 μm in diameter with a current of 3 to 13 nA was used for excavation on the sample in order to expose frozen fluid inclusions (ice) on the crater bottom. The primary beam was rastered to a 50 μm-square and irradiated around the sample surface above the frozen fluid inclusions. The appearance of ice was monitored by secondary ion images of ^1H and ^{16}O using stigmatic ion optics. The depths of excavation on samples reached 15 to 55 μm. During excavation, abrupt electric discharging often occurred because of severe electrostatic charging on the excavation area. In order to minimize the electrostatic charging, the irradiation position of the electron beam was adjusted to the raster area and the immersion lens of the secondary ion optics was continually refocused on the crater bottom during excavation. The excavation time to expose frozen fluid inclusions varied from 0.5 to 8 hours. After we exposed ice, the exposed ice was carefully centered onto the optical axis of the secondary ion optics of the 150 μm-image-field by adjusting the sample position in order to measure oxygen and hydrogen isotopic compositions. We determined sizes of fluid inclusions using the secondary ion images.

The primary beam was adjusted to 3 to 5 μm in diameter with a current of 0.08 to 0.1 nA before isotope analysis, which was smaller in size comparing with that on the excavation process. The primary beam was rastered with 5 to 0 μm in response to the size of exposed ice. The position of the 150 μm diameter contrast aperture and focusing of immersion lens were adjusted to minimize aberrations of secondary ion optics for each element. A

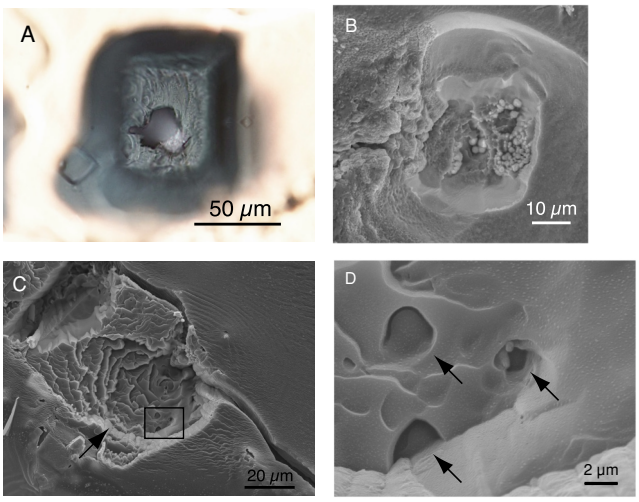

Fig. 7. Representative sputtering crater after isotope analysis. (A) Photomicrograph of the surface of the synthetic halite standard. A negative crystal of a fluid inclusion is observed in the crater bottom. The fluid has been evaporated during takeout from sample chamber of SIMS. (B) Secondary electron image of the negative crystal surface of (A). Small halite grains precipitated during evaporation of the fluid inclusion fluid are observed on the bottom. (C) Secondary electron image of the surface of a Monahans halite crystal. An arrow indicates a sputtering crater of ~50 μm-square. A fluid inclusion analyzed (incl-1) was completely sputtered during analysis, but negative crystals of other three small fluid inclusions (~2 μm) newly appeared in the crater bottom (in black rectangular). (D) Enlarged image of the rectangular area of (C). Arrows indicates negative crystals.

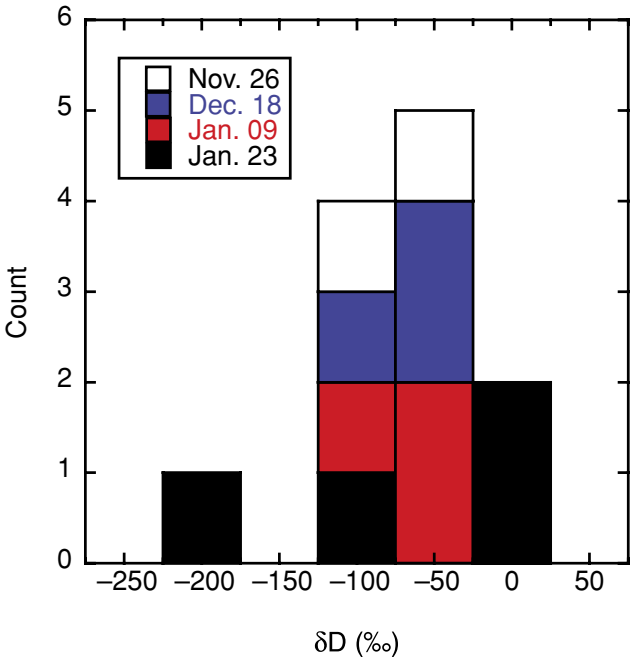

Fig. 8. Reproducibility of hydrogen isotope measurements of fluid inclusion standards.

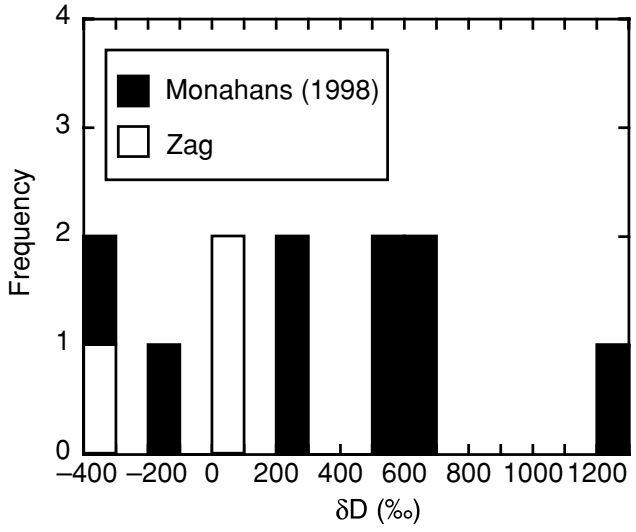

Fig. 9. Variations of hydrogen isotope compositions of fluid inclusions in the Monahans and Zag halite.

field aperture was adjusted to 20 μm square on the 150 μm-image-field.

Negative secondary ions of $^{1}H^{-}$ and $^{2}D^{-}$ were collected sequentially in an electron multiplier for 2 seconds and for 20 seconds, respectively, in peak-jumping mode, at a mass resolution M/ΔM ~ 2300. The sequence was performed for 10 to 30 cycles to calculate the D/H ratio. No interference peaks were observed for $^{1}H^{-}$ and $^{2}D^{-}$ (Fig. 5). Secondary ion intensities of ^{1}H- were ranged over 10 to 600 kilo-count/s.

Negative secondary ions of $^{16}O^{-}$-tail, $^{16}O^{-}$, $^{17}O^{-}$, $^{16}OH^{-}$, and $^{18}O^{-}$ were collected sequentially in an electron multiplier for 2 seconds, 1 second, 10 seconds, 1 second and for 5 seconds, respectively, in peak-jumping mode, at a mass resolution M/ΔM ~ 6300. The sequence was performed for 25 to 120 cycles to calculate the oxygen isotope ratios. No interference peaks were observed for $^{16}O^{-}$ and $^{18}O^{-}$. The interference of $^{17}O^{-}$ was $^{16}OH^{-}$, $^{16}OH^{-}/^{17}O^{-}$ = ~1000, and the interference contribution for $^{17}O^{-}$ peak (2 to 3‰) was corrected by $^{16}O^{-}$-tail/$^{16}O^{-}$ ratio assuming similar peak figures between $^{16}O^{-}$ and $^{16}OH^{-}$ (Fig. 6). Secondary ion intensities of $^{16}O^{-}$ were ranged over 9 to 400 kilo-count/s.

The secondary ions from the excavated crater emitted stably but the intensities changed gradually during the isotope analysis of one spot because the degree of compensation of electrostatic charging by the electron shower shifted gradually as the sputtered crater deepened. In order to compensate the intensity change, linear time inter-

Table 1. Oxygen and hydrogen isotopic compositions of fluid inclusions

Date	Sample	Depth (μm)	Size (μm)	δ^{18}O (‰)	1σ	δ^{17}O (‰)	1σ	Δ^{17}O (‰)	2σ	δD (‰)	2σ
26 Nov. 08	standard	55	15–20	–14.1	6.5	–8.4	6.9	–1.1	7.7	–57.2	9.1
				–36.1	5.6	–20.9	9.2	–2.1	9.6	–96.2	11.4
				16.8	3.3	11.9	6.1	3.2	6.3		
	Monahans (1998)										
	incl-1	40	5–10	60.8	13.9	33.9	17.4	2.3	18.8		
	incl-2	40	5–10	37.2	14.1	3.2	20.3	–16.1	21.6		
	incl-3	40	5–10							549.2	173.0
	incl-4	40	5–10							609.7	108.8
18 Dec. 08	standard	50	15–20	–22.0	6.6	–12.8	6.3	–1.4	7.2	–63.1	8.7
				5.1	4.4	2.3	6.1	–0.3	6.5	–70.5	12.6
				–16.6	5.7	–6.9	6.2	1.7	6.8	–96.5	17.5
	Monahans (1998)										
	incl-5	40	5–10	–4.0	7.5	10.2	13.1	**12.3**	**13.6**	**1204.5**	**54.3**
	incl-6	40	5–10	–3.3	8.7	16.1	8.9	17.8	10.0		
	incl-7	40	5–10	–17.7	5.3	4.5	5.9	13.7	6.5	449.8	48.6
										670.8	97.1
										624.5	73.9
								13.7	**6.5**	***581.7***	***233.1***
	incl-8	40	5	11.2	9.8	23.0	12.5	17.2	13.5	611.5	107.5
				–8.6	13.7	6.3	14.5	10.7	16.1		
								14.0	***4.6***	**611.5**	**107.5**
	incl-9	40	5	40.1	20.8	18.9	19.9	–2.0	22.6	336.3	67.9
										240.1	49.8
								–2.0	**22.6**	***288.2***	***136.0***
8 Jan. 09	standard	30	10–15	–5.5	6.0	–9.2	8.3	–6.3	8.8		
		30	15–20	–3.7	5.5	–2.2	5.3	–0.3	6.0	–35.4	49.7
				–16.9	8.3	–2.0	9.5	6.8	10.4	–124.6	25.2
				–18.6	9.8	–9.8	9.0	–0.2	10.4	–70.0	54.5
	Monahans (1998)										
	incl-10	40	5–10	1.4	4.2	–5.0	7.2	–5.7	7.5	–180.8	59.2
				2.6	4.3	3.2	5.5	1.9	5.9	–11.8	64.4
				–23.2	19.5	5.0	12.5	17.0	16.1	–172.5	73.0
				15.5	4.9	9.6	5.9	1.6	6.4		
								3.7	***9.6***	***–121.7***	***190.6***
	incl-11	40	5							–328.0	59.8
	incl-12	40	5–10	–24.2	14.0	–18.0	18.2	**–5.4**	**19.6**	**291.1**	**98.0**
23 Jan. 09	standard	55	10–15	–14.4	4.1	0.0	8.8	7.5	9.1	–23.2	18.4
				–24.2	3.9	–18.4	5.3	–5.8	5.7	–177.9	29.0
				5.1	7.9	1.0	8.4	–1.7	9.3	–88.0	19.7
										–17.7	19.2
	Zag										
	incl-1	15	5–10	–13.5	7.5	18.4	13.9	**25.4**	**14.4**	**74.5**	**100.1**
	incl-4	45	5–10	45.0	5.5	50.4	10.7	**27.0**	**11.0**	**89.9**	**97.7**
	incl-8	45	5	9.7	7.3	25.5	10.4	20.4	11.1		
	incl-9	45	5	6.5	6.7	6.9	9.4	3.5	10.0		
	incl-10	45	5							–314.4	96.3

Depth: depth from halite surface to inclusion. Size: approximate inclusion size. Reported errors are propagated from analyses. Bold types correspond to inclusions having values for both oxygen and hydrogen isotopes. Italic types correspond to inclusions having duplicate measurements. Italic values correspond to means or standard deviations from duplicate measurements.

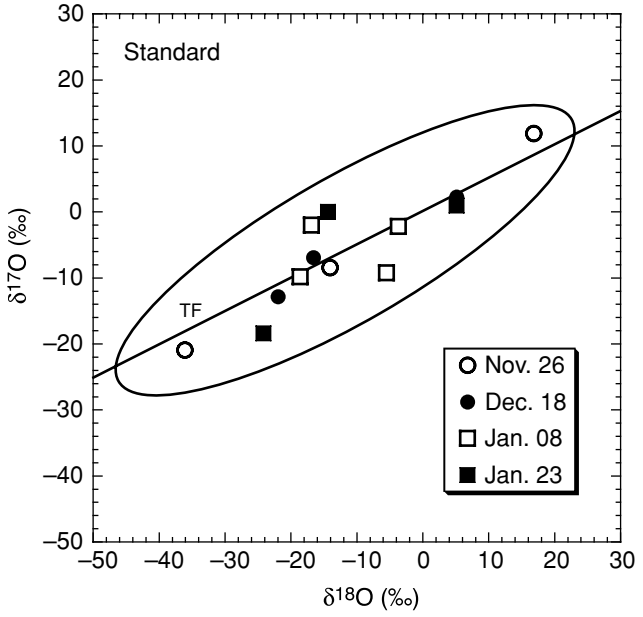

Fig. 10. Reproducibility of oxygen isotope measurements of fluid inclusion standards. Error ellipse indicates 95% confidence. TF: terrestrial fractionation line.

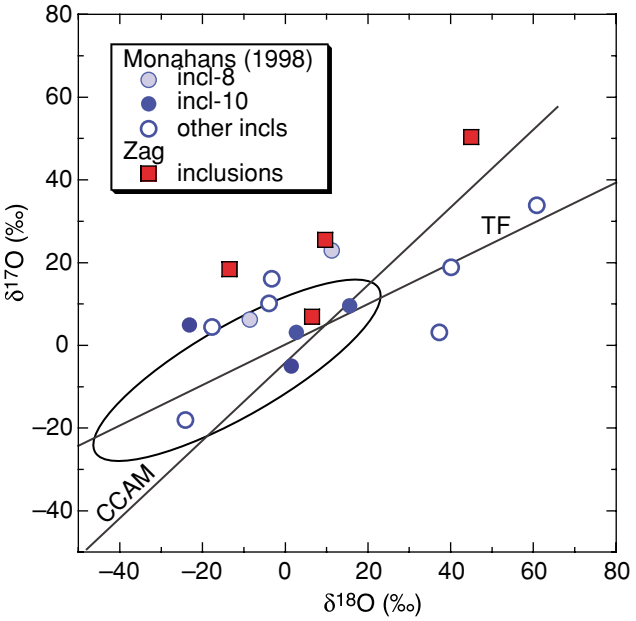

Fig. 11. Three oxygen isotope plots of fluid inclusions in the Monahans and Zag halites. Error ellipse of 95% confidence of standard measurement reproducibility is shown. Duplicate measurements of inclusion #8 and inclusion #10 show that the precision of sample measurements is comparable to the error ellipse. TF: terrestrial fractionation line, CCAM: carbonaceous chondrites anhydrous mineral mixing line.

polation was applied to the secondary ion intensities and isotope ratios were calculated for each cycle. Dead time correction and background noise correction of the electron multiplier were also applied to the secondary ion intensities. The isotope ratios for each cycle were averaged to obtain final isotope ratios of the measurement spot. Representative sputtering craters are shown in Fig. 7.

Results

All data of isotope analysis for asteroidal liquid water are summarized in Table 1. Oxygen and hydrogen isotopic compositions are expressed in δ-units, which are deviations in parts per thousand (per mil, ‰) in the $^{17}O/^{16}O$, $^{18}O/^{16}O$ and D/H ratios from Standard Mean Ocean Water (SMOW):

$$\delta^{17,18}O_{SMOW} = [(^{17,18}O/^{16}O)_{sample}/(^{17,18}O/^{16}O)_{SMOW} - 1] \times 1000,$$

$$\delta D = [(D/H)_{sample}/(D/H)_{SMOW} - 1] \times 1000.$$

Deviation from the terrestrial fractionation line is expressed as $\Delta^{17}O_{SMOW} = \delta^{17}O_{SMOW} - 0.52 \times \delta^{18}O_{SMOW}$.

Hydrogen isotope analysis

Analysis errors expected by count statistics for fluid-inclusion standard were typically about ±20‰ (2σ), which were comparable with standard errors for each measurement of fluid inclusions of Monahans and Zag halite. Figure 8 shows histogram of δD among independent measurements of standards. The histogram ranges from –200‰ to 0‰ and the reproducibility is calculated to be ±90‰ (2σ). The practical reproducibility is about 5 times worse compared with the ideal case. We infer that the degradation of reproducibility results from different degrees of mass fractionation due to variable degrees of electrostatic charged state and the fluctuation at secondary ion emitted area because of insufficient charge compensation on each crater bottom by deep excavation as described above.

Analysis errors for fluid inclusions of Monahans and Zag halite are calculated by standard errors of each measurement and of fluid inclusion standard for the measurement day (Table 1). δD values of fluid inclusions of Monahans and Zag halite range from widely –400 to +1300‰ (Fig. 9). The variation is larger than the reproducibility of standard analysis and the estimated error of each measurement.

Oxygen isotope analysis

Analysis errors expected by counting statistics for fluid-inclusion standard were typically about ±15‰ (2σ), which were comparable with standard errors for each

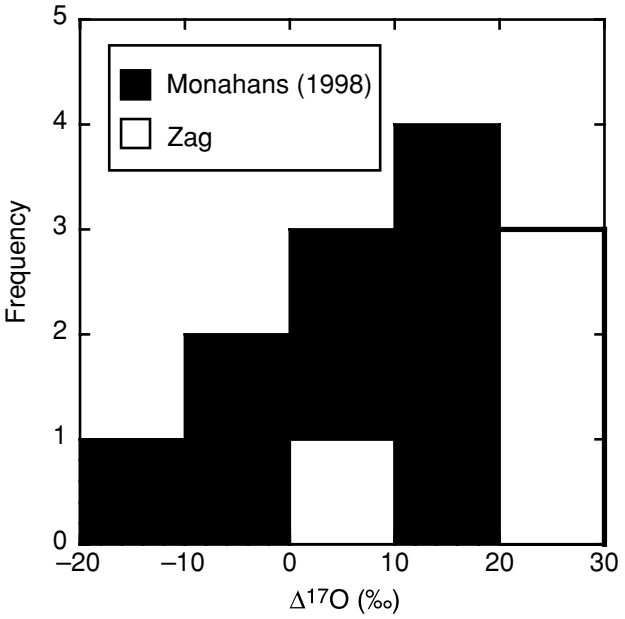

Fig. 12. Variations of mass-independent-fractionation component of oxygen isotope composition of fluid inclusions in the Monahans and Zag halite.

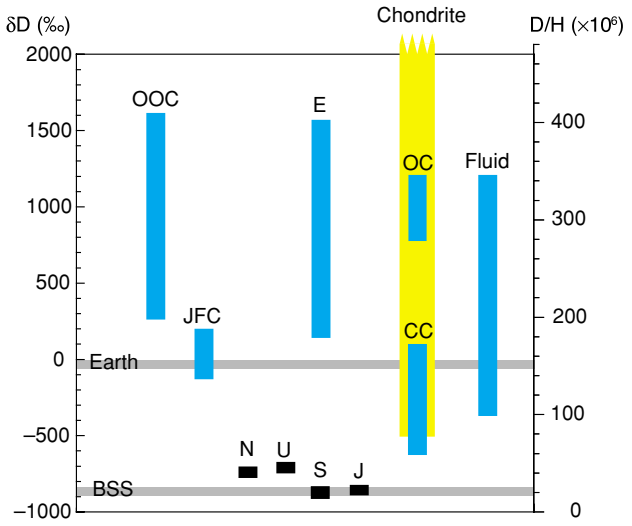

Fig. 13. Distribution of hydrogen isotopic compositions observed in the Solar System. Bulk Solar System (BSS) (Geiss and Gloeckler, 2003; Linsky et al., 2006), Bulk Earth (Earth) (Lecuyer et al., 1998), Jupiter (J) (Lellouch et al., 2001), Saturn (S) (Lellouch et al., 2001), Uranus (U) (Feuchtgruber et al., 2013), Neptune (N) (Feuchtgruber et al., 2013), Enceladus (E) (Waite et al., 2009), Oort-cloud comets (OOC) (Balsiger et al., 1995; Biver et al., 2006; Bockelée-Morvan et al., 1998, 2012; Hutsemékers et al., 2008; Meier et al., 1998; Villanueva et al., 2009), Jupiter-family comets (JFC) (Hartogh et al., 2011; Lis et al., 2013), chondrites (Robert, 2006), estimated compositions of water in carbonaceous (CC) and ordinary (OC) chondrites (Alexander et al., 2012) and fluid inclusion of chondrite (Fluid) (this study).

measurement of fluid inclusions of Monahans and Zag halite. However, on the oxygen three isotope diagram, plots of the standard scattered in a wider range from –40 to +20‰ of $\delta^{18}O$ along the terrestrial mass fractionation line as shown in the error ellipse of 95% confidence (Fig. 10). We infer that the larger error ellipse than estimated errors results from variation of electrostatic charged state of the surface due to deep cratering among measurements as discussed in hydrogen isotope analysis. However, the reproducibility of $\Delta^{17}O$ is calculated to be ±8‰ (2σ), which is comparable with the estimated errors, because of the nature of mass fractionation.

Analysis errors for fluid inclusions of the Monahans and Zag halite are calculated by standard errors of each measurement and of fluid inclusion standard for the measurement day (Table 1). Multiple measurements for single fluid inclusion were successfully collected for two inclusions, incl-8 and incl-10 of Monahans halite. The reproducibility of oxygen isotopic compositions is consistent with those estimated by standards (Fig. 11). Oxygen isotopic compositions of fluid inclusions of Monahans and Zag halite seem to have various degrees of mass-fractionation towards the heavier direction compared with terrestrial ocean water (Fig. 11).

Variations of mass-independent-fractionation component of oxygen isotopic composition ($\Delta^{17}O$) of fluid inclusion of the Monahans and Zag halite range widely from –20 to +30‰ (Fig. 12). The variation clearly shows that the fluid is under disequilibrium for oxygen isotopes among inclusions. The distribution shifts in the ^{16}O-poor direction compared with bulk oxygen isotopic composition of ordinary chondrites (Clayton *et al.*, 1991). The ^{16}O-depletion is larger in the asteroidal aqueous fluid than the most ^{16}O-depleted extraterrestrial magnetite formed by aqueous alteration (Choi *et al.*, 1998).

Discussion

Hydrogen isotopes of the aqueous fluid inclusions ranged from –400 to +1300‰ on the δD scale (Fig. 13). This distribution spans the entire range of aqueously-altered minerals of chondrites and comparable to those of comets and icy satellites of outer planets, but is extremely D-rich compared with outer planets. Oxygen isotopes of the aqueous fluids fractionated mass-independently ranging from –15 to +30‰ in the $\Delta^{17}O$ scale (Fig. 14). The degree of ^{16}O-depletion is larger in the aqueous fluid than the most ^{16}O-depleted astromaterial magnetite formed by aqueous alteration on asteroids identified so far (Choi *et al.*, 1998). The variation of oxygen isotopes of fluid inclusions is unique among solar system

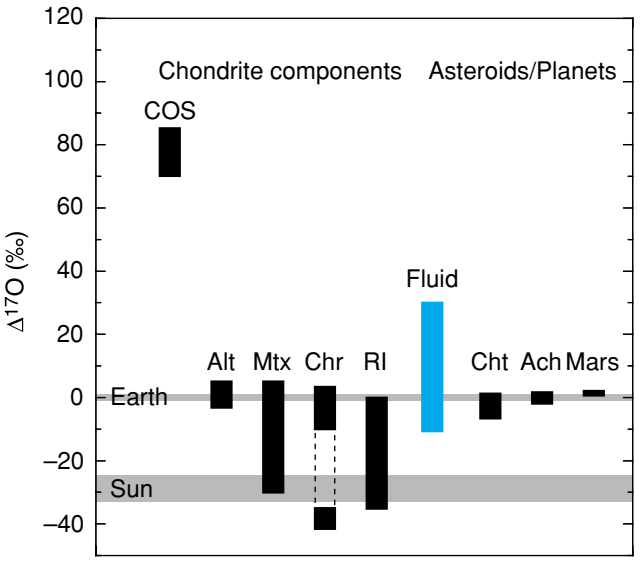

Fig. 14. Distribution of oxygen isotopic compositions observed in the Solar System. Sun (McKeegan et al., 2011), Earth, Mars, achondrite (Ach), chondrite (Cht) (Clayton, 1993), chondrule (Chr), refractory inclusions (RI), chondrite matrix excluding presolar grains (Mtx), aqueous alteration phases of chondrite (Alt) (Yurimoto et al., 2008), cosmic symplectite (COS) (Sakamoto et al., 2007) and fluid inclusion of chondrite (Fluid) (this study).

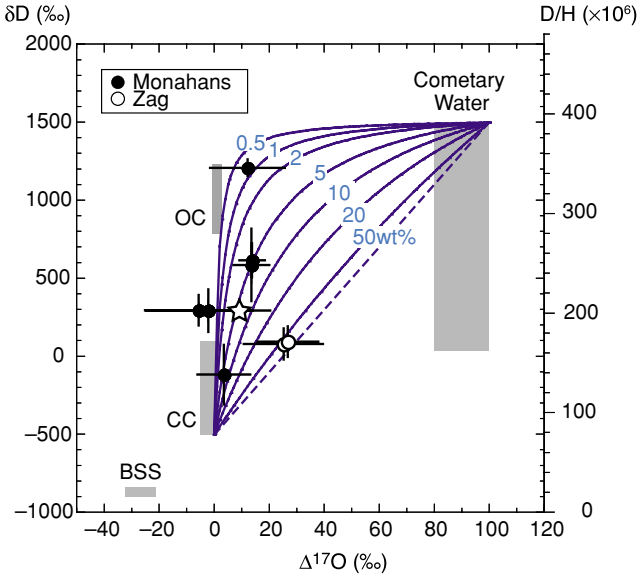

Fig. 15. Relationships of isotopic compositions between hydrogen and oxygen. Open star: average of all measurements shown in Table 1, BSS: bulk solar system, OC: water of ordinary chondrites, CC: water of carbonaceous chondrites, error bars: 2 standard deviations. Water-rock interaction relationships between cometary water and carbonaceous chondrites are shown as blue curves. Water contents of carbonaceous chondrites are parameters and the values are shown on each curve. Isotope fractionation of hydrogen during the interaction is not taken into account because isotopic compositional differences between CC and Cometary water are much larger than the isotopic fractionation factors. Fluid inclusions in Monahans and Zag halite are plotted in the mixing area between CC and Cometary water (reference data from Alexander et al. (2012); Clayton and Mayeda (1999); Clayton et al. (1991); Hartogh et al. (2011); McKeegan et al. (2011); Sakamoto et al. (2007); Yurimoto et al. (2008) and references therein).

objects so far. The highly heterogeneous isotopic compositions between inclusions being heavily fractionated for hydrogen and mass-independently fractionated for oxygen, indicate that aqueous fluids were in isotopic disequilibrium before being trapped in halite.

Isotopic compositions of hydrogen and oxygen in the same fluid were determined for 6 and 2 fluid inclusions from Monahans and Zag halite, respectively, among the total of 17 measured inclusions, and are plotted in δD–Δ^{17}O space in Fig. 15. The average isotopic composition of the 17 inclusions is also plotted.

None of our data are equivalent to isotopic compositions of ordinary chondrite water (Alexander *et al.*, 2012), demonstrating that these fluid inclusion fluids are not related to indigenous ordinary chondrite fluids. The plots are highly scattered in space, but the D-rich fluids tend to be ^{16}O-poor. These highly disequilibrium characteristics are consistent with highly disequilibrium mineralogy of solid inclusions also trapped in these halites, suggesting a relation to water/rock reactions in some carbonaceous chondrites (Zolensky *et al.*, 2013).

Isotopic compositions of water in carbonaceous chondrites are in the range of –500 to +100‰ for δD (Alexander *et al.*, 2012) and –5 to +2‰ for Δ^{17}O (Yurimoto *et al.*, 2008). The halite fluid inclusion brines plot outside the region of estimated carbonaceous chondrite water. Therefore, a more D-rich and ^{16}O-poor source is required for these fluids. Extremely D-rich water has been reported from comets (Villanueva *et al.*, 2009) although D/H composition among comets is highly variable (Hartogh *et al.*, 2011). Another observation of extremely D-rich water is from Enceladus (Waite *et al.*, 2009). It is known that extremely ^{16}O-poor oxygen has a close relationship with cometary water (Sakamoto *et al.*, 2007). Therefore, highly D-rich and ^{16}O-poor water is expected in comets and icy satellites of outer planets (hereafter collectively called "cometary water"). The inferred range of isotopic composition of cometary water is shown in Fig. 15. Plots of fluid inclusion fluids are distributed in a space between lower side of carbonaceous chondrite water and the upper side of cometary water.

Water-rock interaction relationships between cometary water and hydrous carbonaceous chondrite are shown as blue curves in Fig. 15. Water contents of carbonaceous

chondrites are parameters and the values are shown on each curve. Isotope fractionation of hydrogen during the interaction is not taken into account because isotopic composition differences between carbonaceous chondrite water and cometary water are much larger than the isotopic fractionation factors. If water contents of carbonaceous chondrites are small and the proportion of cometary water component is small in the interaction system, the hydrogen isotopic composition of water becomes easily enriched in D from the initial composition by water-rock interaction, whereas oxygen isotopic composition is hardly changed because of buffering by rocky oxygen components. If cometary water and carbonaceous chondrite water is directly interacted, i.e., proportion of rock is small in the system, the change of hydrogen isotopic composition of water becomes proportional to the change of the oxygen isotopic composition.

Calculations indicate that compositions of the Monahans fluids can be explained by results of simple water-rock interaction. This suggests that the halite parent body consist of at least 1–10 wt.% hydrous components, which is consistent with the normal range of carbonaceous chondrites (Alexander *et al*., 2012). Similar calculations indicate that the Zag fluids represent the direct mixing of carbonaceous chondrite water and cometary water. The isotopic compositions of fluid inclusion fluids suggest that the fluids are products of water-rock interaction with cometary water on carbonaceous chondrite parent asteroids.

The cometary water was delivered by impacting comets onto the asteroids. Aqueous fluid formed from the cometary ice percolating into the asteroids. The aqueous fluid reacted with surrounding rock containing phyllosilicates to change the isotopic compositions of the water. The fluid became supersaturated in halites to trap fluid inclusions at ~25°C (Zolensky *et al*., 1999). Some cometary water directly mixed with indigenous water probably formed from dehydrated phyllosilicates or melted interior ice that formed in inner solar system. The precipitated halites were delivered to ordinary chondrite parent asteroids of Monahans and Zag by impacts or cryovolcanoes (Zolensky *et al*., 2013). An alternative isotope mixing model of water components in the solar nebula has been proposed by Jacqueta and Robert (2013).

The water-rock interaction also may occur on ordinary chondrite parent asteroids because enrichments of deuterium in water might occur during thermal processes on ordinary chondrite parent asteroids (Alexander *et al*., 2010) and the chemical compositions are also chondritic. If so, isotopic compositions of ordinary chondrite water may originally resemble carbonaceous chondrite water. However, the particular mineral assemblage and organic components of the solid inclusions observed in Monahans and Zag halite require carbonaceous chondrite-like asteroids for the water-rock interaction sites (Zolensky *et al*., 2013). In any case, because chondritic and cometary waters are believed to have originated in the inner solar nebula (Alexander *et al*., 2012; Robert, 2006) and outer solar nebula to molecular cloud (Greenberg, 1998), respectively, the isotopic compositions of the halite fluids suggest that dynamic delivery and accretion of water originated throughout the solar system and in the parent molecular cloud onto planetesimals was a fundamental mechanism in the evolution of present planetary water. Isotopic composition of lunar rock water (Greenwood *et al*., 2011) suggests that the global water mixing or delivery processes in the solar system continued at least until the time of the Moon's formation and early evolution.

Conclusions

We determined hydrogen and oxygen isotopic compositions of asteroidal aqueous fluids (in this case brines) by secondary ion mass spectrometry (SIMS) equipped with a cryogenic apparatus for sample cooling. The asteroidal aqueous fluids were trapped in halite found in two ordinary chondrites of Monahans (H5) and Zag (H3-6). The cryogenic apparatus cooled fluid inclusion fluids down to about –190°C and the fluid was frozen. The frozen fluid inclusion fluids were exposed in vacuum to prepare for SIMS.

Hydrogen isotopes of the fluid inclusion fluids ranged from –400 to +1300‰ on the δD scale relative to SMOW. Oxygen isotopes of the fluid inclusion fluids fractionated mass-independently ranging from –20 to +30‰ in the Δ^{17}O scale relative to SMOW. The distribution of isotopic composition of the both elements larger than the entire range of aqueously-altered minerals of chondrites. The wide variations of hydrogen and oxygen isotopic compositions indicate that isotope equilibria were under way in the asteroidal fluid before trapping into halite.

The isotopic distribution on δD vs. Δ^{17}O space suggests that mixing between inner solar system water representing chondritic water and outer solar system water representing cometary water occurred on planetesimals in the early solar system and water-rock interaction proceeded on the planetesimals to produce inner planetary water. We propose that this is a fundamental mechanism in the evolution of present planetary water. Variations of isotopic compositions of water among planets, asteroids, comets, icy satellites, and other solar system objects would be results of this fundamental mechanism.

Acknowledgments—We thank Hideo Kitajima for his assistance with the cryo-stage. We thank François Robert, Marc Chaussidon and Shogo Tachibana for their constructive reviews and suggestions. This study was partly supported by a Monkasho Grant (H.Y.) and the NASA Cosmochemistry Program (M.Z.). We thank Edwin Thompson for bringing the halite in

Zag to our attention, and Everett Gibson for obtaining the Monahans samples for NASA.

References

Alexander, C. M. O. D., Newsome, S. D., Fogel, M. L., Nittler, L. R., Busemann, H. and Cody, G. D. (2010) Deuterium enrichments in chondritic macromolecular material—Implications for the origin and evolution of organics, water and asteroids. *Geochim. Cosmochim. Acta* **74**, 4417–4437.

Alexander, C. M. O. D., Bowden, R., Fogel, M. L., Howard, K. T., Herd, C. D. K. and Nittler, L. R. (2012) The provenances of asteroids, and their contributions to the volatile inventories of the terrestrial planets. *Science* **337**, 721–723.

Balsiger, H., Altwegg, K. and Geiss, J. (1995) D/H and $^{18}O/^{16}O$ ratio in the hydronium ion and in neutral water from in situ ion measurements in comet Halley. *J. Geophys. Res.* **100**, 5827–5834.

Biver, N., Bockelée-Morvan, D., Crovisier, J., Lis, D. C., Moreno, R., Colom, P., Henry, F., Herpin, F., Paubert, G. and Womack, M. (2006) Radio wavelength molecular observations of comets C/1999 T1 (Mc Naught-Hartley), C/2001 A2 (LINEAR) and 153/P Ikeya-Zhang. *Astron. Astrophys.* **449**, 1255–1270.

Bockelée-Morvan, D., Gautier, D., Lis, D. C., Young, K., Keene, J., Phillips, T., Owen, T., Crovisier, J., Goldsmith, P. F., Bergin, E. A., Despois, D. and Wootten, A. (1998) Deuterated water in comet C/1996 B2 (Hyakutake) and its implication for the origin of comets. *Icarus* **133**, 147–162.

Bockelée-Morvan, D., Biver, N., Swinyard, B., de Val-Borro, M., Crovisier, J., Hartogh, P., Lis, D. C., Moreno, R., Szutowicz, S., Lellouch, E., Emprechtinger, M., Blake, G. A., Courtin, R., Jarchow, C., Kidger, M., Küppers, M., Rengel, M., Davis, G. R., Fulton, T., Naylor, D., Sidher, S. and Walker, H. (2012) Herschel measurements of the D/H and $^{16}O/^{18}O$ ratios in water in the Oort-cloud comet C/2009 P1 (Garradd). *Astron. Astrophys.* **544**, L15.

Bogard, D., Garrison, D. and Masarik, J. (2001) The Monahans chondrite and halite: ^{39}Ar–^{40}Ar age, solar gases, cosmic-ray exposure ages, and parent body regolith neutron flux and thickness. *Meteorit. Planet. Sci.* **36**, 107–122.

Butner, H. M., Charnley, S. B., Ceccarelli, C., Rodgers, S. D., Pardo, J. R., Parise, B., Cernicharo, J. and Davis, G. R. (2007) Discovery of interstellar heavy water. *Astrophys. J.* **659**, L137–L140.

Choi, B.-G., McKeegan, K. D., Krot, A. N. and Wasson, J. T. (1998) Extreme oxygen-isotope compositions in magnetite from unequilibrated ordinary chondrites. *Nature* **392**, 577–579.

Clayton, R. N. (1993) Oxygen isotopes in meteorites. *Annu. Rev. Earth Planet. Sci.* **21**, 115–149.

Clayton, R. N. and Mayeda, T. K. (1999) Oxygen isotope studies of carbonaceous chondrites. *Geochim. Cosmochim. Acta* **63**, 2089–2104.

Clayton, R. N., Mayeda, T. K., Goswami, J. N. and Olsen, E. J. (1991) Oxygen isotope studies of ordinary chondrites. *Geochim. Cosmochim. Acta* **55**, 2317–2337.

Feuchtgruber, H., Lellouch, E., Orton, G., de Graauw, T., Vandenbussche, B., Swinyard, B., Moreno, R., Jarchow, C., Billebaud, F., Cavalié, T., Sidher, S. and Hartogh, P. (2013) The D/H ratio in the atmospheres of Uranus and Neptune from Herschel-PACS observations. *A&A* **551**.

Geiss, J. and Gloeckler, G. (2003) Isotopic composition of H, He and Ne in the protosolar cloud. *Space Sci. Rev.* **106**, 3–18.

Greenberg, J. M. (1998) Making a comet nucleus. *Astron. Astrophys.* **330**, 375–380.

Greenwood, J. P., Itoh, S., Sakamoto, N., Warren, P., Taylor, L. and Yurimoto, H. (2011) Hydrogen isotope ratios in lunar rocks indicate delivery of cometary water to the Moon. *Nature Geoscience* **4**, 79–82.

Hartogh, P., Lis, D. C., Bockelée-Morvan, D., Val-Borro, M. D., Biver, N., Küppers, M., Emprechtinger, M., Bergin, E. A., Crovisier, J., Rengel, M., Moreno, R., Szutowicz, S. and Blake, G. A. (2011) Ocean-like water in the Jupiter-family comet 103P/Hartley 2. *Nature* **478**, 218–220.

Hayashi, C., Nakazawa, K. and Nakagawa, Y. (1985) Formation of the solar system. *Protostars and Planets II* (Black, D. C. and Matthews, M. S., eds.), 1100–1153, University of Arizona Press, Tucson.

Hutsemékers, D., Manfroid, J., Jehin, E., Zucconi, J.-M. and Arpigny, C. (2008) The $^{16}OH/^{18}OH$ and OD/OH isotope ratios in comet C/2002 T7 (LINEAR). *Astron. Astrophys.* **490**, L31–L34.

Jacqueta, E. and Robert, F. (2013) Water transport in protoplanetary disks and the hydrogen isotopic composition of chondrites. *Icarus* **223**, 722–732.

Kuramoto, K. and Yurimoto, H. (2005) Oxygen isotopic heterogeneity in the solar system: the molecular cloud origin hypothesis and its implications for meteorites and the planets. *Chondrites and the Protoplanetary Disk* **341** (Krot, A. N., Scott, E. R. D. and Reipurth, B., eds.), 181–192, ASP Conference Series.

Kusakabe, M. and Matsuhisa, Y. (2008) Oxygen three-isotope ratios of silicate reference materials determined by direct comparison with VSMOW-oxygen. *Geochem. J.* **42**, 309–317.

Lecuyer, C., Gillet, P. and Robert, F. (1998) The hydrogen isotope composition of seawater and the global water cycle. *Chem. Geol.* **145**, 249–261.

Lellouch, E., Bézard, B., Fouchet, T., Feuchtgruber, H., Encrenaz, T. and Graauw, T. D. (2001) The deuterium abundance in Jupiter and Saturn from ISO-SWS observations. *A&A* **370**, 610–622.

Linsky, J. L., Draine, B. T., Moos, H. W., Jenkins, E. B., Wood, B. E., Oliveira, C., Blair, W. P., Friedman, S. D., Gry, C., Knauth, D., Kruk, J. W., Lacour, S., Lehner, N., Redfield, S., Shull, J. M., Sonneborn, G. and Williger, G. M. (2006) What is the total deuterium abundance in the local galactic disk? *Astrophys. J.* **647**, 1106–1124.

Lis, D. C., Biver, N., Bockelée-Morvan, D., Hartogh, P., Bergin, E. A., Blake, G. A., Crovisier, J., Val-Borro, M. D., Jehin, E., Küppers, M., Manfroid, J., Moreno, R., Rengel, M. and Szutowicz, S. (2013) A herschel study of D/H in water in the Jupiter-family comet 45P/Honda-Mrkos-Pajdušková and prospects for D/H measurements with CCAT. *Astrophys. J. Lett.* **774**, L3.

Lyons, J. R. and Young, E. D. (2005) CO self-shielding as the

origin of oxygen isotope anomalies in the early solar nebula. *Nature* **435**, 317–320.

McKeegan, K. D., Kallio, A. P. A., Heber, V. S., Jarzebinski, G., Mao, P. H., Coath, C. D., Kunihiro, T., Wiens, R. C., Nordholt, J. E., Moses, R. W., Jr., Reisenfeld, D. B., Jurewicz, A. J. G. and Burnett, D. S. (2011) The oxygen isotopic composition of the Sun inferred from captured solar wind. *Science* **332**, 1528–1532.

Meier, R., Owen, T. C., Matthews, H. E., Jewitt, D. C., Bockelée-Morvan, D., Biver, N., Crovisier, J. and Gautier, D. (1998) A determination of the HDO/H2O ratio in comet C/1995 O1 (Hale-Bopp). *Science* **279**, 842–844.

Nassau, K. (1983) *The Physics and Chemistry of Color*. Wiley Publishing Co.

Robert, F. (2006) Solar system deuterium/hydrogen ratio. *Meteorites and the Early Solar System II* (Lauretta, D. S. and McSween, H. Y., eds.), 341–351, University of Arizona Press, Tucson.

Rubin, A. E., Zolensky, M. E. and Bodnar, R. J. (2002) The halite-bearing Monahans (1998) and Zag meteorite breccias: Shock metamorphism, thermal metamorphism and aqueous alteration on the H-chondrite parent body. *Meteorit. Planet. Sci.* **37**, 125–142.

Sakamoto, N., Seto, Y., Itoh, S., Kuramoto, K., Fujino, K., Nagashima, K., Krot, A. N. and Yurimoto, H. (2007) Remnants of the early solar system water enriched in heavy oxygen isotopes. *Science* **317**, 231–233.

Villanueva, G. L., Mumma, M. J., Bonev, B. P., DiSanti, M. A., Gibb, E. L., Böhnhardt, H. and Lippi, M. (2009) A sensitive search for deuterated water in comet 8P/Tuttle. *Astrophys. J.* **690**, L5–L9.

Waite, J. H., Jr., Lewis, W. S., Magee, B. A., Lunine, J. I., McKinnon, W. B., Glein, C. R., Mousis, O., Young, D. T., Brockwell, T., Westlake, J., Nguyen, M. J., Teolis, B. D., Niemann, H. B., McNutt, R. L., Jr., Perry, M. and Ip, W. H. (2009) Liquid water on Enceladus from observations of ammonia and ^{40}Ar in the plume. *Nature* **460**, 487–490.

Whitby, J., Burgess, R., Turner, G., Gilmour, J. and Bridges, J. (2000) Extinct ^{129}I in halite from a primitive meteorite: Evidence for evaporite formation in the early solar system. *Science* **288**, 1819–1821.

Yurimoto, H. and Kuramoto, K. (2004) Molecular cloud origin for the oxygen isotope heterogeneity in the solar system. *Science* **305**, 1763–1766.

Yurimoto, H., Krot, A. N., Choi, B.-G., Aleon, J., Kunihiro, T. and Brearley, A. J. (2008) Oxygen isotopes of chondritic components. *Rev. Mineral. Geochem.* **68**, 141–186.

Yurimoto, H., Itoh, S., Zolensky, M. E., Kusakabe, M. and Karen, A. (2010) Isotopic compositions of fluid inclusions in halites from ordinary chondrites. *Meteorit. Planet. Sci.* **45**, A222.

Zolensky, M. E., Bodnar, R. J., Gibson, E. K., Jr., Nyquist, L. E., Reese, Y., Shih, C.-Y. and Wiesmann, H. (1999) Asteroidal water within fluid inclusion-bearing halite in an H5 chondrite, Monahans (1998). *Science* **285**, 1377–1379.

Zolensky, M. E., Bodnar, R. J., Schwandt, C. and Yang, S. V. (2000) Halite minerals in the Monahans (1998) and Zag H chondrite regolith breccias. *Lunar Planet. Sci.* **XXXI**.

Zolensky, M., Fries, M., Bodnar, R., Yurimoto, H., Itoh, S., Steele, A., Mikouchi, T., Hagiya, K., Ohsumi, K., Le L. and Rahman, Z. (2013) Early solar system cryovolcanics in the laboratory. *Meteorit. Planet. Sci.* **48**, #5200.